

Supplementary information

Synthesis of a platinacycle: Determination of the structure and examination of the photophysical properties based on DFT calculations

Ken Motohara,^a Kazuhiro Kado,^a Taichi Sotani,^a Dayang Zhou,^b Takeyuki Suzuki,^b Hiromitsu Sogawa,^a Fumio Sanda^{*a}

^a Department of Chemistry and Materials Engineering, Faculty of Chemistry, Materials and Bioengineering, Kansai University
3-3-35 Yamate-cho, Suita, Osaka 564-8680, Japan

^b Comprehensive Analysis Center, SANKEN, Osaka University, Ibaraki, Osaka 567-0047, Japan

* Corresponding Author: sanda@kansai-u.ac.jp

EXPERIMENTAL

Measurements

¹H and ¹³C NMR spectra were recorded on JEOL JNM-ECS400, JNM-ECZ400, JNM-ECA600 and BRUEKR AVANCE III 700 spectrometers. IR spectra were measured on a JASCO FT/IR-4100 spectrophotometer. Platinacycle 1 was purified with a Japan Analytical Industry preparative HPLC system equipped with JAIGEL-1H (exclusion limit 1,000) and JAIGEL-2H (exclusion limit 5,000). MALDI-TOF MS spectra were measured on BRUKER microflex LT mass spectrometer [matrix: dithranol, mass range: 1–2200; mode, linear (positive), laser power 60–80%]. Number-average molecular weight (M_n) and dispersity (D) values of polymers were determined with an SEC system (Shodex GPC KD-G × 2, Shodex TSK-GEL α-M C0053 × 2, JASCO CO-965, UV-2075 Plus, RI-930, PU-980, DG-980-50) using *N,N*-dimethylformamide (DMF) containing LiBr (10 mM) as an eluent calibrated by polystyrene standards at 40 °C. UV-vis absorption spectra were measured in a quartz cell (optical distance:1 cm) using a JASCO V-550 spectrometer. Photoluminescence spectra were measured on a HITACHI F-7000 spectrometer. XRD spectra were measured on a BRUKER D2 PHASER with Cu-K α radiation.

Materials

All reagents were commercially obtained from FUJIFILM Wako Pure Chemical Corporation, Tokyo Chemical Industry Co., Ltd., NACALAI TESQUE, INC., Sigma-Aldrich Japan, KANTO CHEMICAL CO., INC and WATANABE CHEMICAL INDUSTRIES, LTD., EIWEISS Chemical Corporation. The solvents used for synthesis under argon were dried over molecular sieves 4A 1/16, and degassed by argon bubbling. The other reagents were used as received without purification.

Synthesis of Dinuclear Platinacycle **1** and Mononuclear Non-Macrocyclic Pt Complex **1'**.

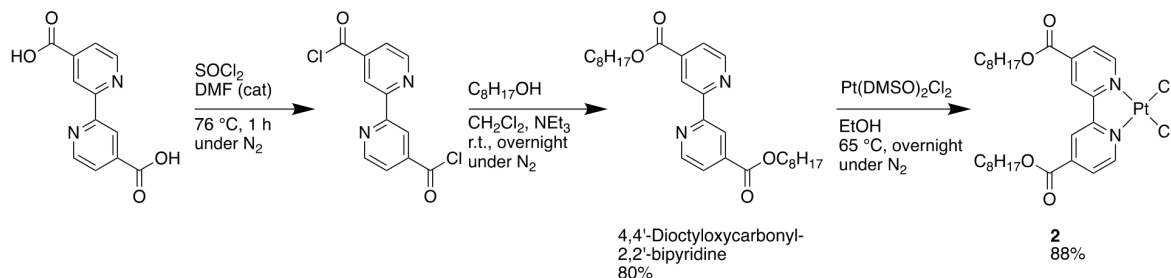
They were synthesized according to Schemes S1–S5. The synthetic procedures are described below.

4,4'-Diocetylloxycarbonyl-2,2'-bipyridine.^{S1} The title compound was synthesized according to Scheme S1. 2,2'-Bipyridine-4,4'-dicarboxylic acid (4.50 g, 18.4 mmol) was fed into a reaction vessel. DMF (40.0 μ L) and SOCl_2 (20.0 mL, 258 mmol) were fed into the vessel, and the resulting mixture was stirred at 76 °C under N_2 for 1 h. DMF and residual SOCl_2 were removed by evaporation under vacuum to obtain 2,2'-bipyridine-4,4'-dicarbonyl chloride as a brown residue. The reaction vessel was cooled to –76 °C, then a mixture of CH_2Cl_2 (150 mL), NEt_3 (10 mL), and 1-octanol (7.5 mL, 48.0 mmol) was fed to the vessel. The resulting mixture was stirred at room temperature under N_2 overnight. The solvents were removed by evaporation under vacuum, and CH_2Cl_2 was added to the residue. Solvent-insoluble amine salts were removed by filtration, and the filtrate was washed with satd. NaCl aq. The organic layer was separated from the aqueous layer, dried over anhydrous MgSO_4 , and concentrated on a rotary evaporator. The residue was purified by silica gel column chromatography eluted with hexane/ethyl acetate = 5/2 (v/v) to obtain the title compound as a yellow solid (6.90 g, 14.7 mmol). Yield = 80%. ^1H NMR (400 MHz, CDCl_3): δ 0.88 (t, J = 6.86 Hz, 6H, $-\text{CH}_3 \times 2$), 1.22–1.46 (m, 20H, $-(\text{CH}_2)_5\text{CH}_3 \times 2$), 1.80 (t, J = 11.4 Hz, 4H, $-\text{OCH}_2\text{CH}_2-\times 2$), 4.36–4.40 (m, 4H, $-\text{OCH}_2-\times 2$), 7.90 (d, J = 3.2 Hz, 2H, Ar), 8.86 (t, J = 8.2 Hz, 2H, Ar), 9.08 (s, 2H, Ar) ppm.

[**4,4'-Diocetylloxycarbonyl-2,2'-bipyridine]PtCl₂** (**2**).^{S2} The title compound was synthesized according to Scheme S1. 4,4'-Diocetylloxycarbonyl-2,2'-bipyridine (1.97 g, 4.20 mmol) and *cis*- $\text{Pt}(\text{DMSO})_2\text{Cl}_2$ (1.72 g, 4.20 mmol) were fed into a reaction vessel. EtOH (150 mL) was fed into

the vessel, and the resulting mixture was stirred at 65 °C under N₂ for 24 h. The solvent was removed by evaporation. The residue was purified by silica gel column chromatography eluted with CH₂Cl₂ to obtain **2** as an orange solid (2.70 g, 3.70 mmol). Yield = 88%. ¹H NMR (400 MHz, CDCl₃): δ 0.88 (t, *J* = 11.9 Hz, 6H, –CH₃ × 2), 1.22–1.46 (m, 20H, –(CH₂)₅CH₃ × 2), 1.83 (t, *J* = 21.0 Hz, 4H, –OCH₂CH₂– × 2), 4.40 (t, *J* = 13.7 Hz, 4H, –OCH₂– × 2), 7.91 (d, *J* = 10.5 Hz, 2H, Ar), 8.50 (s, 2H, Ar), 9.40 (d, *J* = 12.5 Hz, 2H, Ar) ppm.

Scheme S1. Synthesis of Pt Complex 2



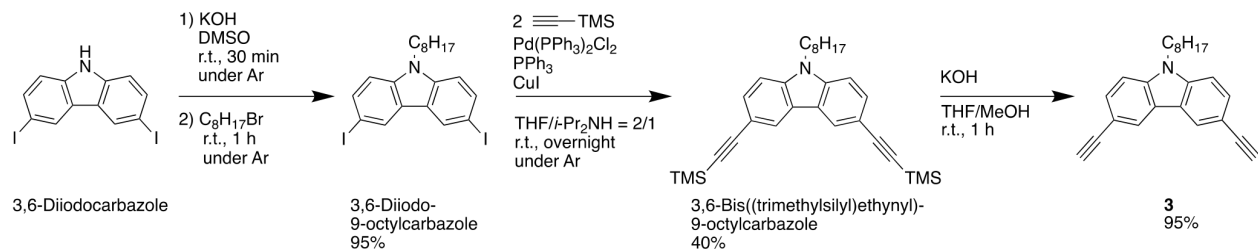
3,6-Diiodo-9-octylcarbazole.^{S3} The title compound was synthesized according to Scheme S2. A solution of 3,6-diiodocarbazole in DMSO (750 mmol, 20 mL, 15.0 mmol) was added to a solution of KOH (5.07 g, 90.0 mmol) in DMSO (20 mL), and the resulting mixture was stirred for 30 min. Then 1-bromooctane (2.85 mL, 16.0 mmol) was added to the mixture, and the resulting mixture was poured into water (300 mL) to precipitate a white solid. It was collected by filtration, and purified by recrystallization with hexane to obtain the title compound as a white solid (7.59 g, 14.3 mmol). Yield = 95%. ¹H NMR (400 MHz, CDCl₃): δ 0.88 (t, *J* = 17.6 Hz, 3H, –CH₃), 1.22–1.29 (m, 10H, –(CH₂)₅CH₃), 1.76–1.85 (m, 2H, >NCH₂CH₂–), 4.22 (t, *J* = 14.6 Hz, 2H, >NCH₂–), 7.18 (d, *J* = 8.23 Hz, 2H, Ar), 7.77 (d, *J* = 9.61 Hz, 2H, Ar), 8.33 (s, 2H, Ar) ppm.

3,6-Bis((trimethylsilyl)ethynyl)-9-octylcarbazole.^{S3} The title compound was synthesized according to Scheme S2. 3,6-Diido-9-octylcarbazole (3.90 g, 7.34 mmol), Pd(PPh₃)Cl₂ (41.9 mg,

0.070 mmol), PPh₃ (18.0 mg, 0.070 mmol) and CuI (13.3 mg, 0.070 mmol) were dissolved in a mixture of THF (35 mL) and NEt₃ (35 mL). Trimethylsilylacetylene (2.1 mL, 14.85 mmol) was added to the mixture, and the resulting mixture was stirred at 50 °C for 48 h. The solvent was removed by evaporation to obtain a brown oil. It was dissolved in diethyl ether (200 mL), and the resulting solution was washed with satd. NH₄Cl aq. The organic layer was separated from the aqueous layer, dried over anhydrous MgSO₄, and concentrated on a rotary evaporator to obtain a brown oil. It was purified by silica gel column chromatography eluted with hexane/CH₂Cl₂ = 8/1 (v/v) to obtain the title compound as a yellow oil (1.52 g, 2.94 mmol). Yield = 40%. ¹H NMR (400 MHz, CDCl₃): δ 0.27 (s, 18H, –Si(CH₃)₃ × 2), 0.88 (t, *J* = 17.6 Hz, 3H, –CH₃), 1.22–1.29 (m, 10H, –(CH₂)₅CH₃), 1.76–1.85 (m, 2H, >NCH₂CH₂–), 4.22 (t, *J* = 14.6 Hz, 2H, >NCH₂–), 7.18 (d, *J* = 8.23 Hz, 2H, Ar), 7.77 (d, *J* = 9.61 Hz 2H, Ar), 8.33 (s, 2H, Ar) ppm.

3,6-Diethynyl-9-octylcarbazole (3).^{S4} The title compound was synthesized according to Scheme S2. 3,6-Bis((trimethylsilyl)ethynyl)-9-octyl-carbazole (0.670 g, 1.35 mmol) was fed into a reaction vessel. THF (10 mL) and KOH solution in MeOH (405 mM, 10 mL, 4.05 mmol) was added to the vessel, and the resulting mixture was stirred at room temperature for 2 h. The solvent was removed by evaporation. The residue was dissolved in CH₂Cl₂ (200 mL), and the resulting solution was washed with satd. NaCl aq. The organic layer was separated from the aqueous layer, dried over anhydrous MgSO₄, and concentrated on a rotary evaporator to obtain **3** as a yellow oil (0.42 g, 1.28 mmol). Yield = 95 %. ¹H NMR (400 MHz, CDCl₃): δ 0.88 (t, *J* = 13.7 Hz, 3H, –CH₃), 1.22–1.31 (m, 10H, –(CH₂)₅CH₃), 1.80–1.86 (m, 2H, >NCH₂CH₂–), 3.08 (s, 2H, ≡CH × 2), 4.27 (t, *J* = 14.2 Hz, 2H, >NCH₂–), 7.32 (d, *J* = 8.23 Hz, 2H, Ar), 7.59 (d, *J* = 8.70 Hz, 2H, Ar), 8.22 (s, 2H, Ar) ppm.

Scheme S2. Synthesis of 3

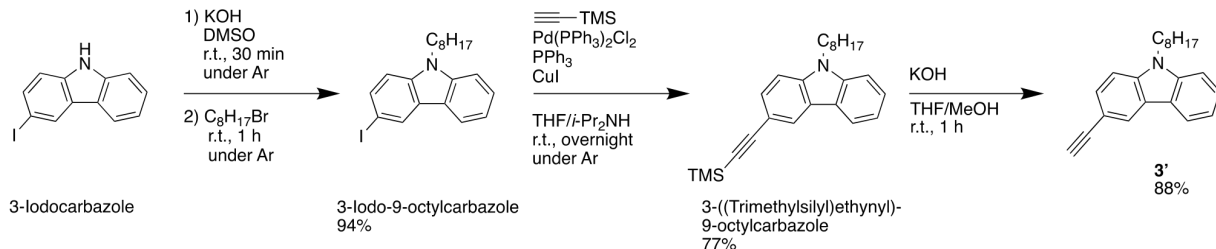


3-Iodo-9-octylcarbazole.^{S5} The title compound was synthesized from 3-iodocarbazole, KOH and 1-bromooctane (Scheme S3) in a manner similar to 3,6-diido-9-octylcarbazole. The product was directly used in the next step without purification. Yield: 94%. ^1H NMR (400 MHz, $CDCl_3$): δ 0.88 (t, J = 24.7 Hz, 3H, $-\text{CH}_3$), 1.22–1.44 (m, 10H, $-(CH_2)_5\text{CH}_3$), 1.80–1.86 (m, 2H, $>\text{NCH}_2\text{CH}_2-$), 4.57 (t, J = 14.6 Hz, 2H, $>\text{NCH}_2-$), 7.18 (d, J = 15.5 Hz, 1H, Ar), 7.22 (d, J = 8.23 Hz, 1H, Ar), 7.38 (d, J = 8.23 Hz, 1H, Ar), 7.50 (t, J = 5.95 Hz, 1H, Ar), 7.70 (d, J = 1.83 Hz, 1H, Ar), 8.05 (d, J = 8.70 Hz, 1H, Ar), 8.39 (s, 1H, Ar) ppm.

3-((Trimethylsilyl)ethynyl)-9-octylcarbazole.^{S6} The title compound was synthesized from 3-iodo-9-octylcarbazole and trimethylsilylacetylene (Scheme S3) in a manner similar to 3,6-bis((trimethylsilyl)ethynyl)-9-octylcarbazole. The product was purified by silica gel column chromatography eluted with hexane/ $CH_2\text{Cl}_2$ = 5/1 (v/v) to give the title compound as a yellow oil. Yield = 77%. ^1H NMR (400 MHz, $CDCl_3$): δ 0.29 (s, 9H, $-\text{Si}(\text{CH}_3)_3$), 0.85 (t, J = 17.4 Hz, 3H, $-\text{CH}_3$), 1.23–1.36 (m, 10H, $-(CH_2)_5\text{CH}_3$), 1.82–1.89 (m, 2H, $>\text{NCH}_2\text{CH}_2-$), 4.28 (t, J = 14.8 Hz, 2H, $>\text{NCH}_2-$), 7.22 (d, J = 7.78 Hz, 1H, Ar), 7.31 (d, J = 8.23 Hz, 1H, Ar), 7.40 (d, J = 8.23 Hz, 1H, Ar), 7.46 (t, J = 8.23 Hz, 1H, Ar), 7.58 (d, J = 1.37 Hz, 1H, Ar), 8.07 (d, J = 15.1 Hz, 2H, Ar), 8.24 (s, 1H, Ar) ppm.

3-Ethynyl-9-octylcarbazole (3').^{S6} The title compound was synthesized from 3-((trimethylsilyl)ethynyl)-9-octylcarbazole (Scheme S3) in a manner similar to **3**. The product was directly used in the next step without purification. Yield = 88%. ¹H NMR (400 MHz, CDCl₃): δ 0.85 (t, J = 13.7 Hz, 3H, -CH₃), 1.23–1.36 (m, 10H, -(CH₂)₅CH₃), 1.82–1.89 (m, 2H, >NCH₂CH₂-), 3.11 (s, 1H, ≡CH), 4.28 (t, J = 14.2 Hz, 2H, >NCH₂-), 7.22 (d, J = 7.78 Hz, 1H, Ar), 7.33 (d, J = 8.23 Hz, 1H, Ar), 7.40 (d, J = 8.23 Hz, 1H, Ar), 7.47 (t, J = 15.1 Hz, 1H, Ar), 7.60 (d, J = 8.69 Hz, 1H, Ar), 8.08 (d, J = 7.78 Hz, 1H, Ar), 8.26 (s, 1H, Ar) ppm.

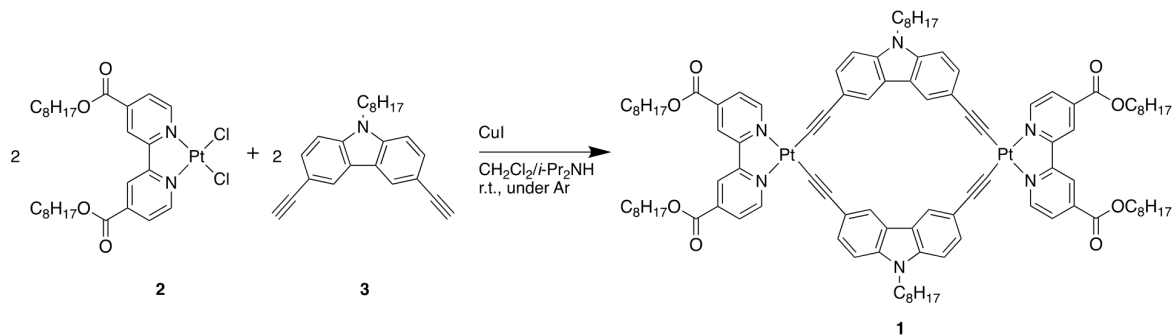
Scheme S3. Synthesis of 3'



Synthesis Platinacycle 1. The title complex was synthesized according to Scheme S4. Typical procedure: Compounds **2** (440 mg, 0.60 mmol) and **3** (230 mg, 0.60 mmol) were fed into a reaction vessel filled with argon. CH₂Cl₂ (400 mL) and *i*-Pr₂NH (200 mL) were fed into the vessel, and a solution of CuI in *i*-Pr₂NH was added. The resulting mixture was stirred under Ar atmosphere at room temperature overnight. The solvent was removed by evaporation to obtain a black solid. It was dissolved in CH₂Cl₂ (500 mL), and the resulting solution was washed with satd. NH₄Cl aq. The organic layer was separated from the aqueous layer, dried over anhydrous MgSO₄, and concentrated on a rotary evaporator to obtain a black solid. It was purified by preparative HPLC to obtain **1** as a black solid. Yield = max 15%. No mp was observed up to 300 °C. ¹H NMR (400 MHz, CDCl₃): δ 0.84–0.95 (m, 18H, -CH₃ × 6), 1.25–2.07 (m, 72H, -(CH₂)₆CH₃ × 6), 4.11–4.46 (m, 12H, >NCH₂- × 2, -OCH₂- × 4), 7.30–10.14 (m, 24H, Ar) ppm. The assignment is described

in Fig. 1. ^{13}C NMR (175 MHz, CDCl_3): δ 13.9, 22.4, 25.4, 27.4, 28.1, 29.0, 31.7, 43.2, 66.5, 83.8, 103.5, 107.7, 118.7, 122.5, 122.6, 125.1, 126.5, 129.9, 138.8, 139.9, 151.5, 157.0, 163.2 ppm. IR(KBr): 2916, 2114, 1726, 1473, 1319, 1257, 1134, 1018, 953, 886, 813, 758, 708, 643, 582, 515 cm^{-1} . MALDI-TOF MS: m/z calcd for $\text{C}_{104}\text{H}_{127}\text{N}_6\text{O}_8\text{Pt}_2$ [$\text{M}+\text{H}]^+$: 1977.90, found: 1978.45.

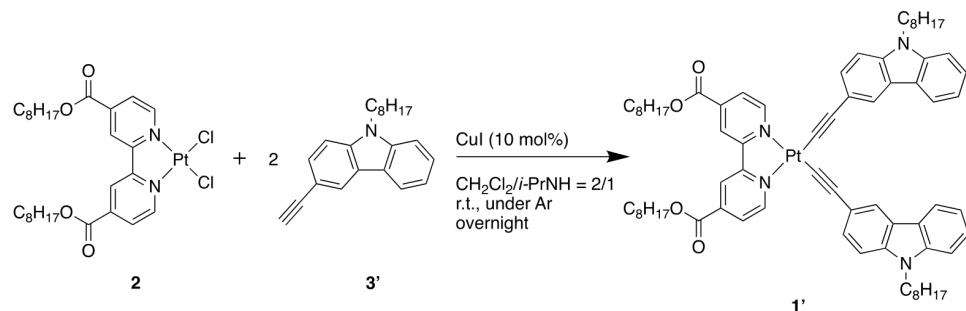
Scheme S4. Synthesis of 1 by Dehydrochlorination Coupling of 2 and 3.



Synthesis of Mononuclear Non-Macrocyclic Platinum Complex 1'. The title complex was synthesized according to Scheme S5. Compounds **2** (478 mg, 0.650 mmol), **3'** (395 mg, 1.30 mmol) and CuI (11.4 mg, 0.060 mmol) were fed into a reaction vessel filled with argon. CH_2Cl_2 (20 mL) and *i*-Pr₂NH (10 mL) were fed into the vessel, and the resulting mixture was stirred at room temperature overnight. The solvent was removed by evaporation. It was dissolved in CH_2Cl_2 , and the resulting solution was washed with satd. NH₄Cl aq. The organic layer was separated, and dried over anhydrous MgSO₄ and concentrated on a rotary evaporator to obtain a black solid. It was purified by silica gel column chromatography eluted with hexane/ CH_2Cl_2 = 1/5 (v/v) and then CH_2Cl_2 to obtain **1'** as a black solid (247 mg, 0.195 mmol). Yield = 30%. Mp = 75–77 °C. ^1H NMR (400 MHz, CDCl_3): δ 0.86–0.90 (m, 12H, $-\text{CH}_3 \times 4$), 1.25–1.43 (m, 40H, $-(\text{CH}_2)_5\text{CH}_3 \times 4$), 1.61–1.63 (t, J = 6.40 Hz, 4H, $-\text{OCH}_2\text{CH}_2-\times 2$), 1.86–1.89 (m, 4H, $>\text{CH}_2\text{CH}_2-\times 2$), 4.09–4.12 (t, J = 10.3 Hz, 4H, $>\text{NCH}_2-\times 2$), 4.26–4.29 (t, J = 14.6 Hz, 4H, $-\text{OCH}_2-\times 2$), 7.17–7.21 (d, J = 15.9 Hz, 2H, Ar), 7.28–7.30 (d, J = 8.23 Hz, 2H, Ar), 7.34–7.37 (d, J = 8.23 Hz, 2H, Ar), 7.40–7.44 (t,

J = 15.1 Hz, 2H, Ar), 7.58–7.61 (dd, *J* = 10.1, 1.37 Hz, 2H, Ar), 8.01–8.03 (d, *J* = 6.86 Hz, 1.37 Hz, 2H, Ar), 8.01 (d, *J* = 7.76 Hz, 2H, Ar), 8.17 (s, 2H, Ar), 8.41 (s, 2H, Ar) 10.0 (d, *J* = 5.49 Hz, 2H, Ar) ppm. ^{13}C NMR (175 MHz, CDCl_3): δ 14.1, 22.6, 25.8, 27.4, 28.4, 29.4, 31.8, 43.2, 66.8, 108.0, 108.5, 118.7, 120.6, 122.2, 122.4, 122.7, 123.9, 125.4, 127.0, 130.5, 138.9, 140.6, 156.6, 163.6 ppm. IR(KBr): 2925, 2853, 2360, 2113, 1726, 1596, 1463, 1315, 1258, 1137, 1054, 967, 883, 802, 761, 615, 572, 543, 511 cm^{-1} . MALDI-TOF MS (*m/z*) calcd for $\text{C}_{72}\text{H}_{89}\text{N}_4\text{O}_4\text{Pt} [\text{M}+\text{H}]^+$; 1268.65, found: 1269.12.

Scheme S5. Synthesis of **1'**



Computations

All computational calculations were performed with the Gaussian 16 program,^{S7} ES64L-G16 Rev C.01, using the DFT method with ω B97X-D functional in conjunction with basis sets, 6-31G* for H, C, N, O, and LANL2DZ for Pt, running on the supercomputer systems, Academic Center for Computing and Media Studies, Kyoto University. The simulated UV-vis absorption spectrum was illustrated using GaussView 6. The MO shapes were illustrated using Avogadro^{S8} version 1.2.0.

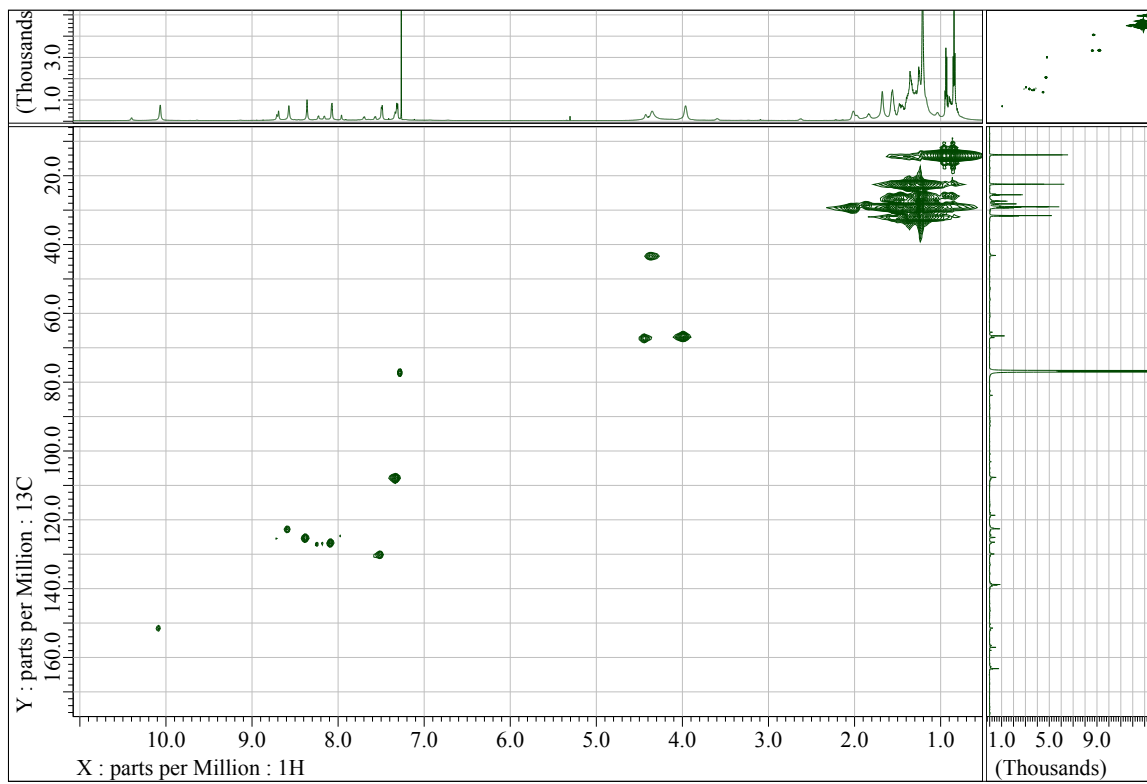


Fig. S1 HMQC (600 MHz) spectrum of **1** measured in CDCl_3 .

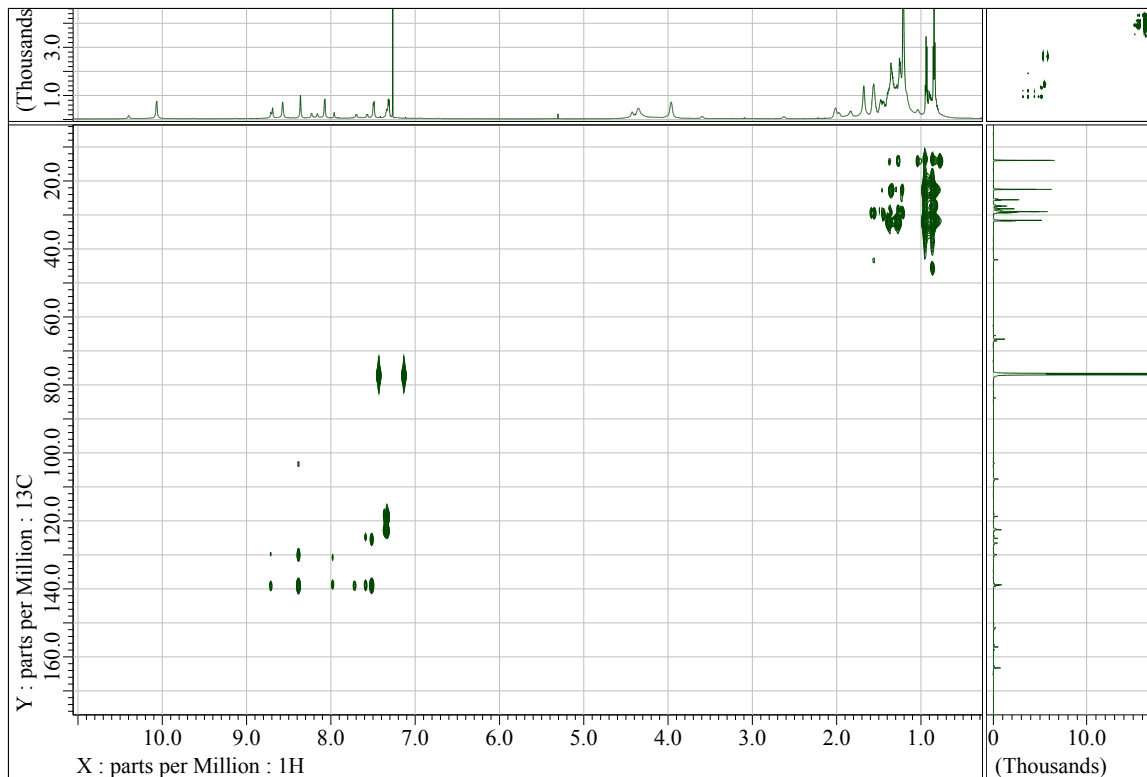


Fig. S2 HMBC (600 MHz) spectrum of **1** measured in CDCl_3 .

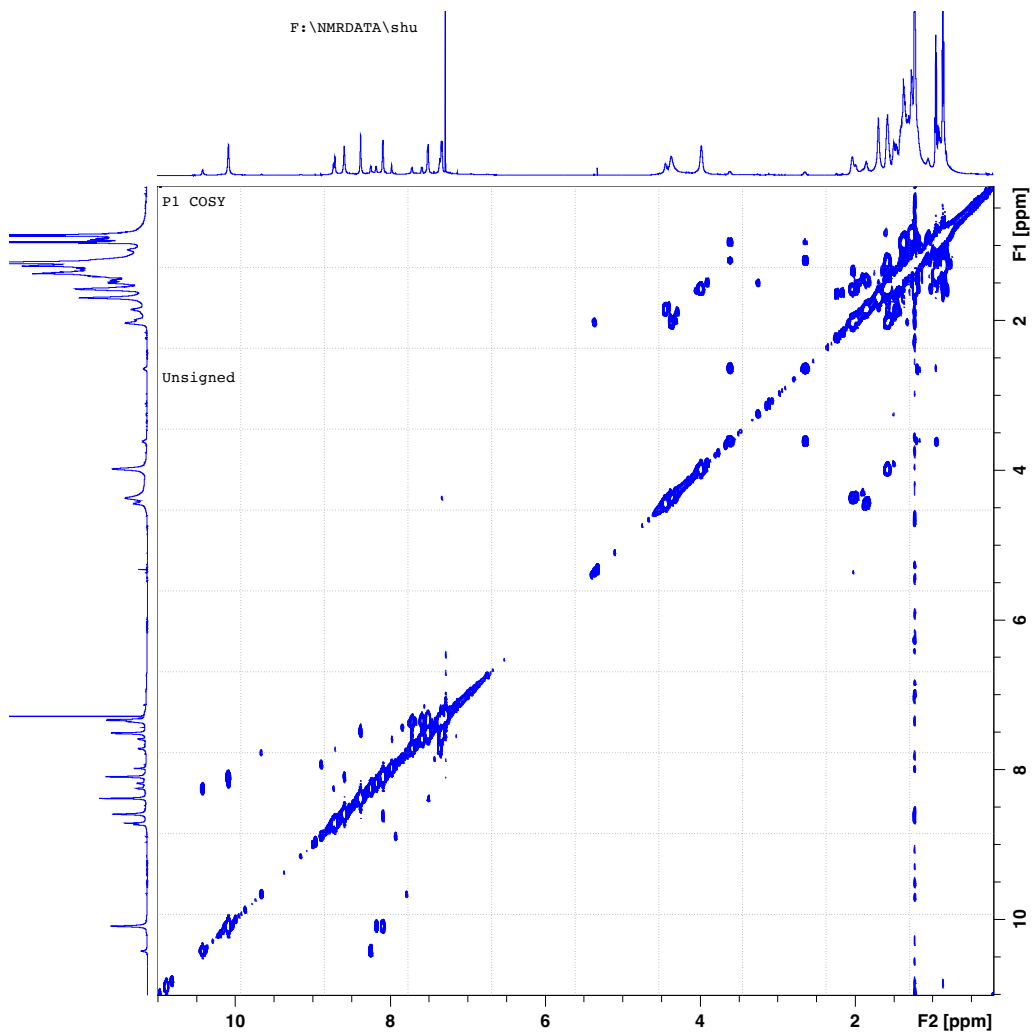


Fig. S3 ^1H - ^1H COSY (700 MHz) spectrum of **1** measured in CDCl_3 .

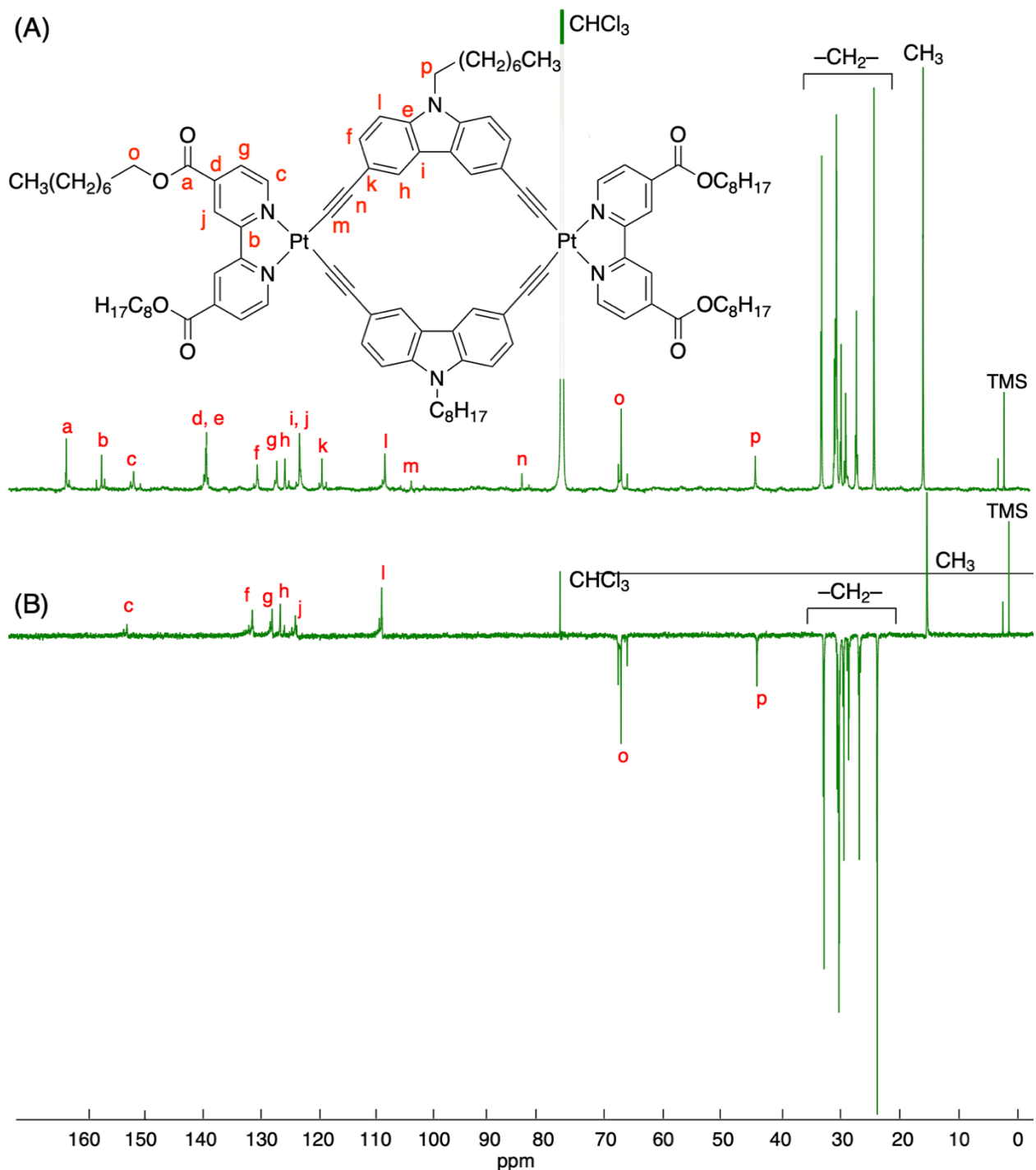


Fig. S4 (A) ^{13}C NMR and (B) DEPT 135 (175 MHz) spectra of **1** measured in CDCl_3 .

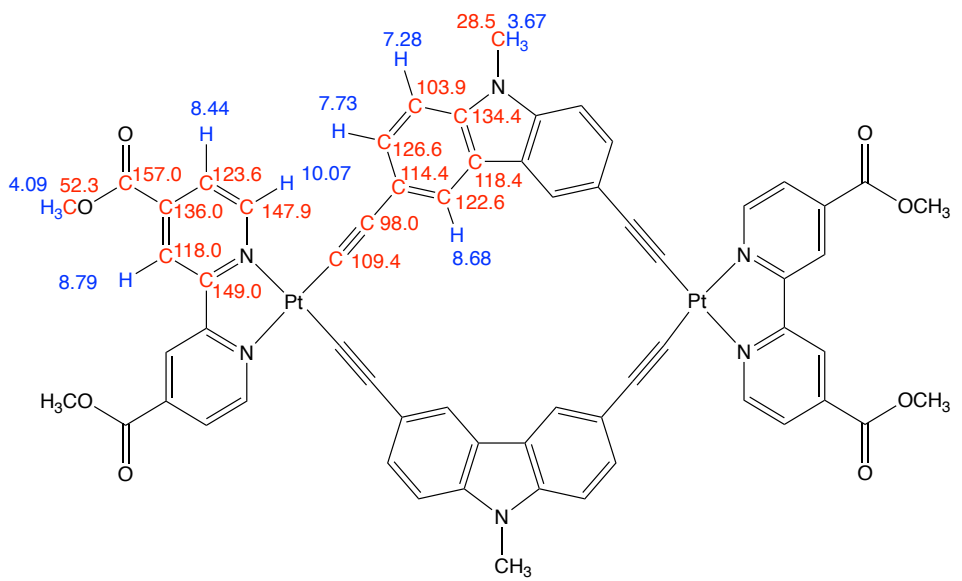


Fig. S5 Chemical shifts of ¹H (blue) and ¹³C (red)-NMR spectra of **1** simulated by the DFT GIAO method [ω B97XD/6-31G* (C, H, N, O)-LANL2DZ (Pt)] using SCRF-IEFPCM (solvent CHCl₃).

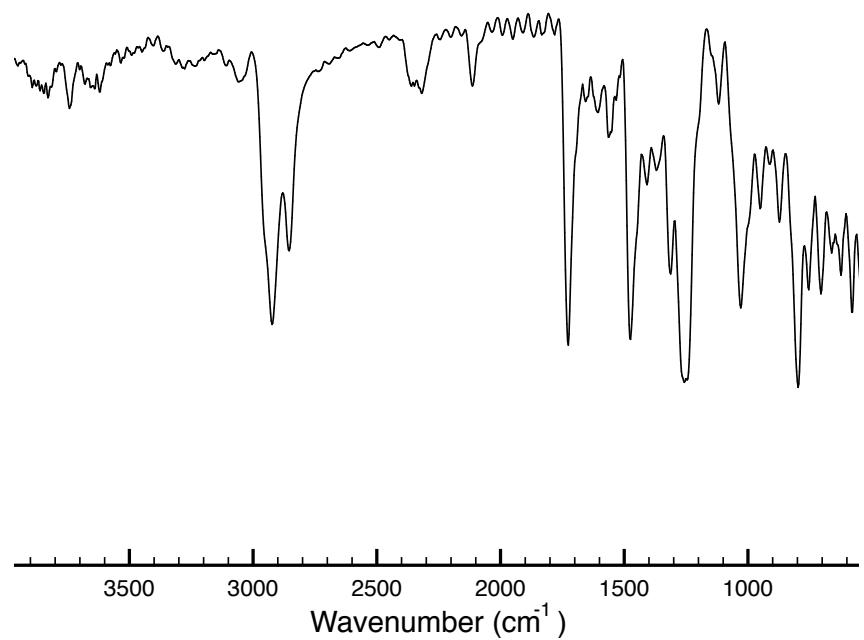


Fig. S6 IR spectrum of **1** measured by the KBr pellet method.

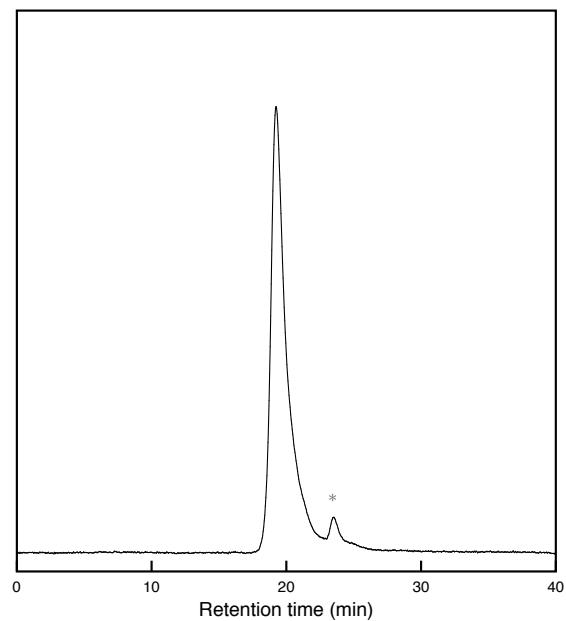


Fig. S7 SEC trace of **1** eluted with LiBr (10 mM) solution in DMF calibrated by polystyrene standards at 40 °C (* ghost peak).

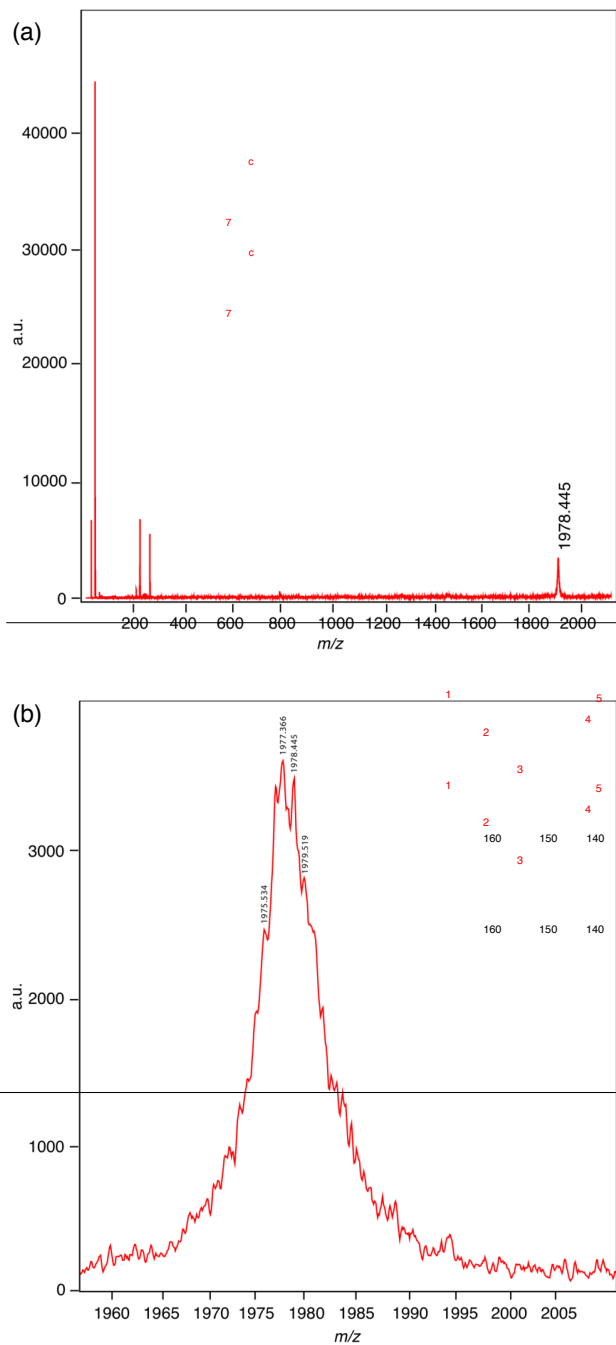


Fig. S8 (a) MALDI-TOF MS chart of **1** (exact mass of $[M+H]^+ = 1977.90$) measured by positive linear mode using dithranol as a matrix. (b) Expanded chart at a range of 1960–2005 m/z .

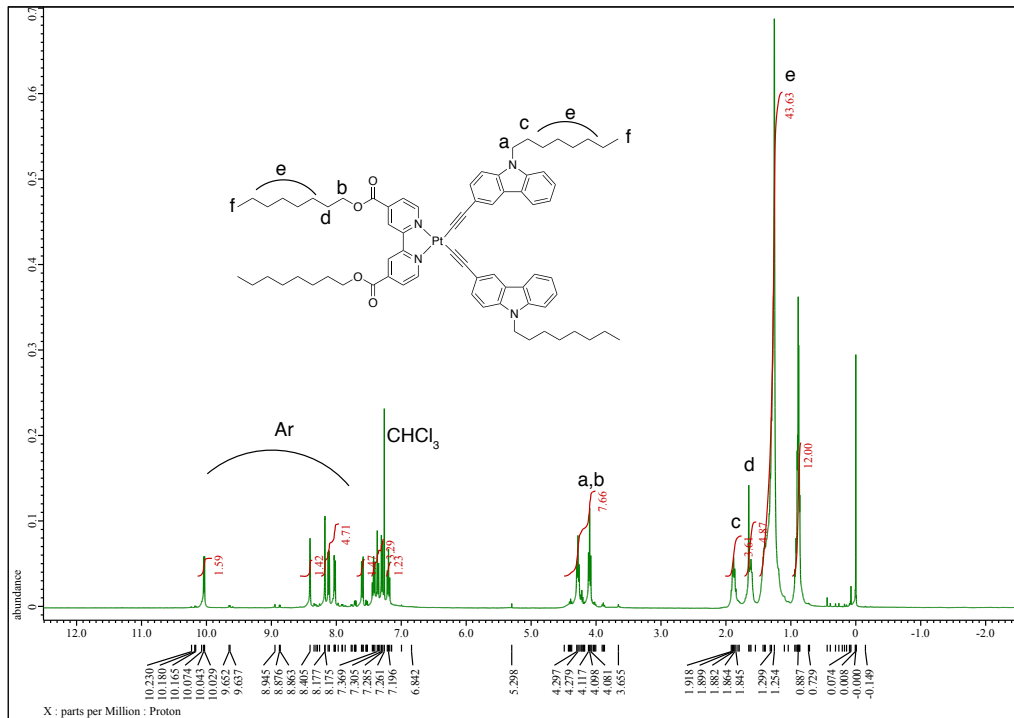


Fig. S9 ^1H NMR (400 MHz) spectrum of **1'** measured in CDCl_3 .

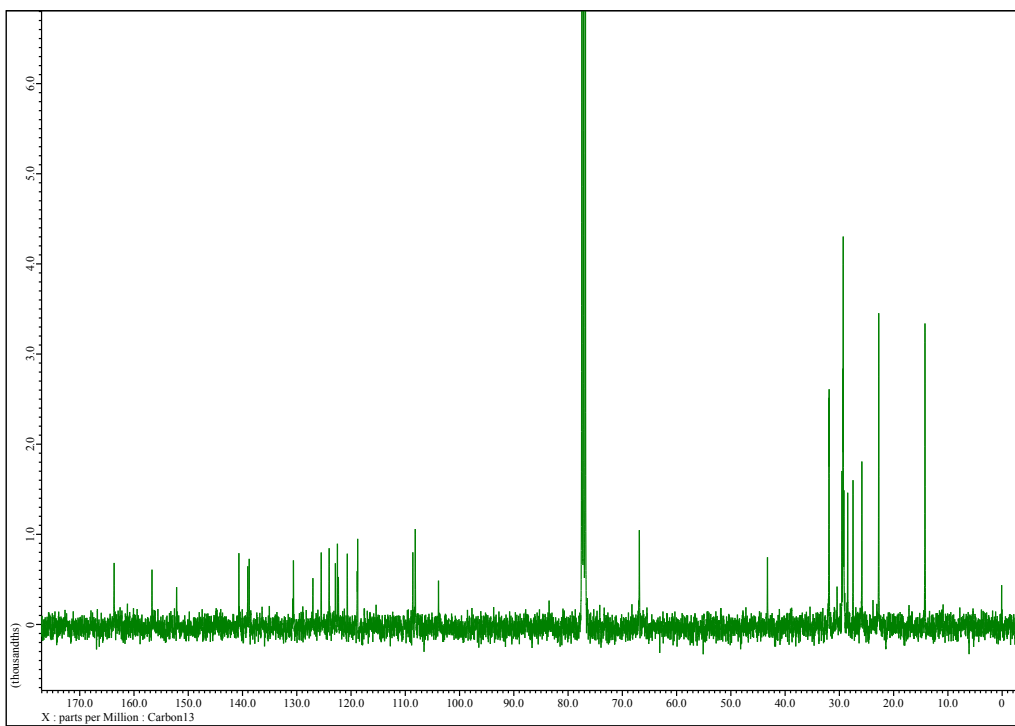


Fig. S10 ^{13}C NMR (100 MHz) spectrum of **1'** measured in CDCl_3 .

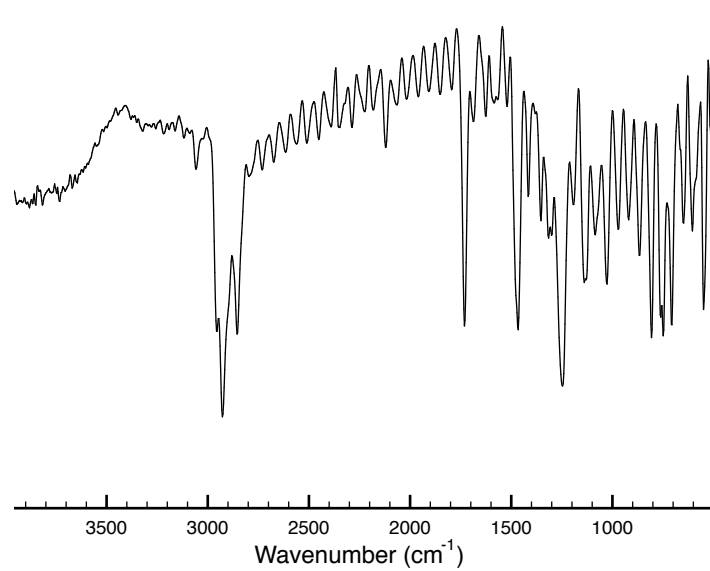


Fig. S11 IR spectrum of **1'** measured by the KBr pellet method.

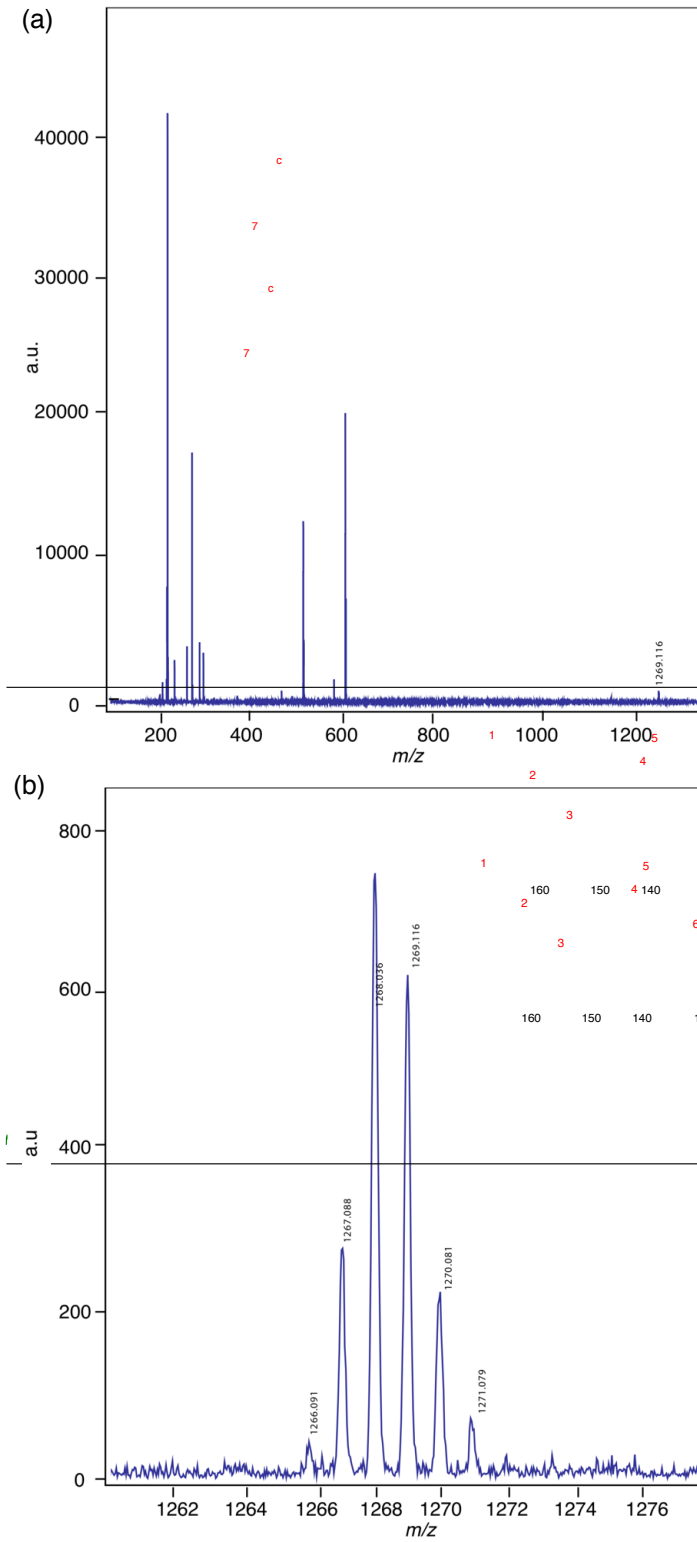


Fig. S12 (a) MALDI-TOF MS chart of **1'** (exact mass = 1267.65) measured by positive linear mode using dithranol as a matrix. (b) Expanded chart at 1260–1278 m/z .

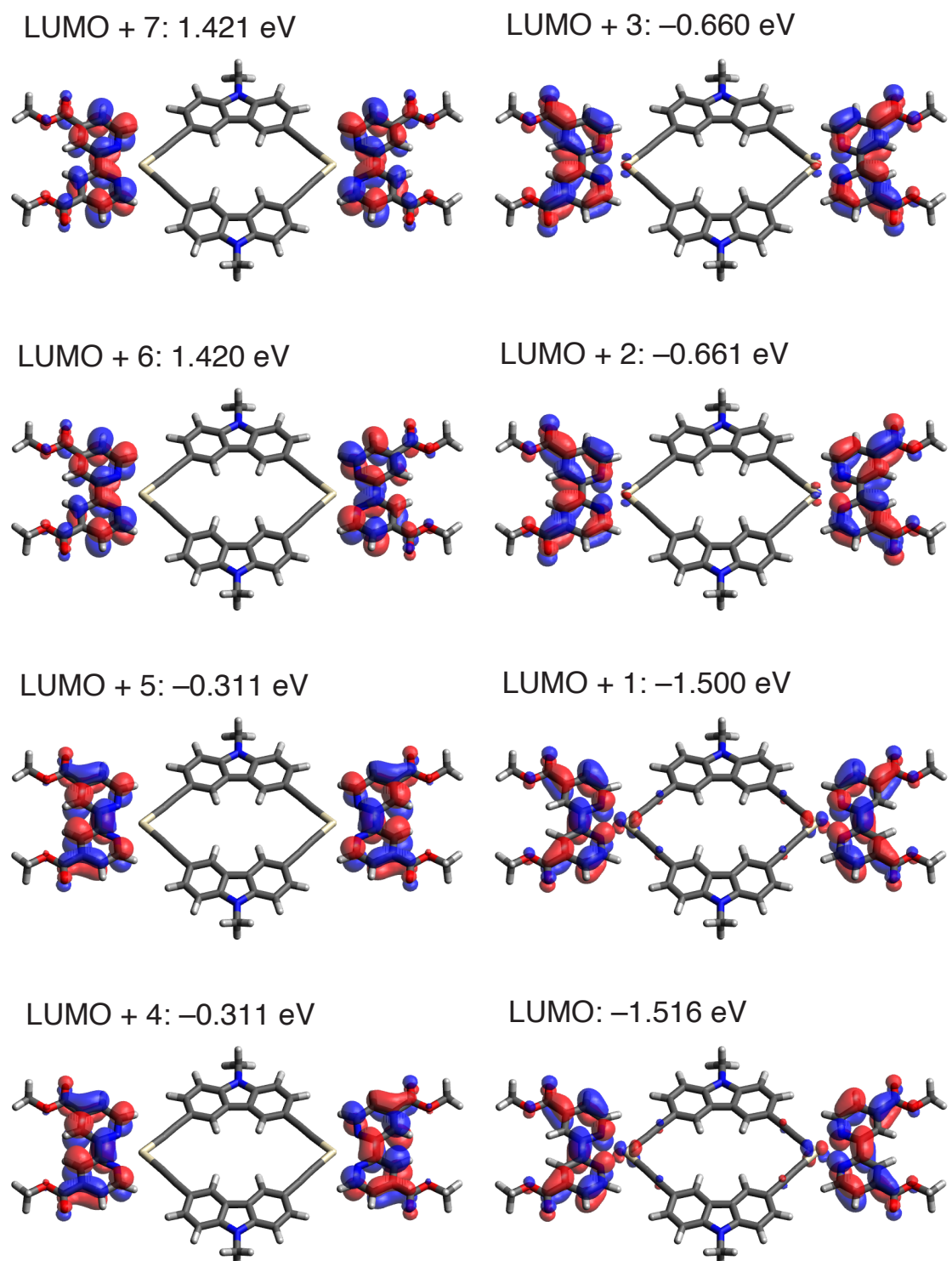


Fig. S13 Shapes and energy levels from LUMO + 7 to LUMO of **1-CH₃** according to the results obtained by the DFT calculations [ω B97XD/6-31G* (H, C, N, O)-LANL2DZ (Pt)].

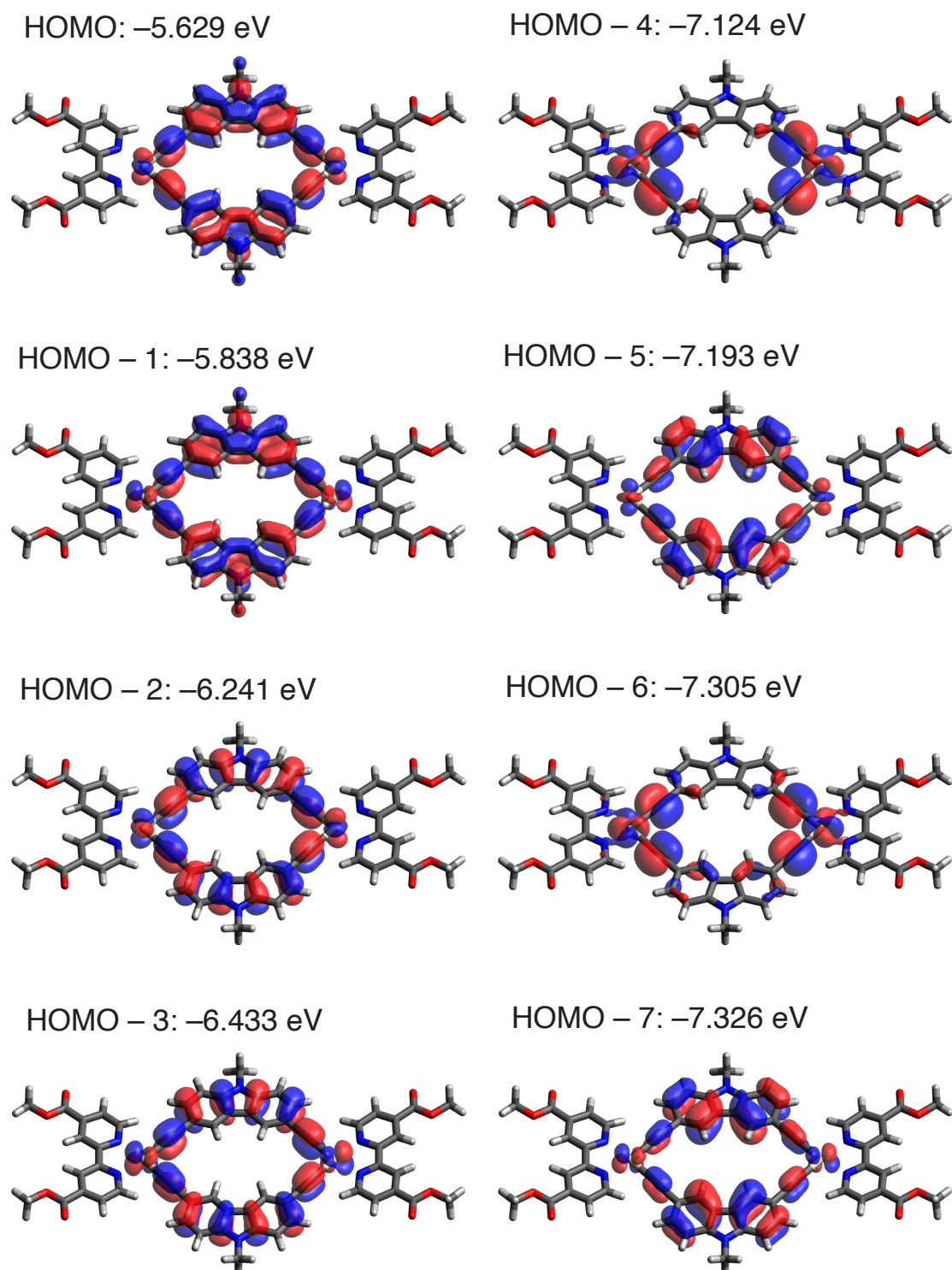


Fig. S14 Shapes and energy levels from HOMO to HOMO – 7 of **1-CH₃** according to the results obtained by the DFT calculations [ω B97XD/6-31G* (H, C, N, O)-LANL2DZ (Pt)].

Data of excitations obtained by the TD-DFT calculation of 1-CH₃

Excited state, spin multiplicity-symmetry, excitation energy (eV, nm), oscillator strength f (intensity of absorption), square spin eigen value, orbitals excited from → to, coefficient of the wavefunction for each excitation. **The texts in red are important data concerning the main absorption depicted in Fig. 5.**

Correspondence of orbital numbers

286: LUMO + 7	282: LUMO + 3
285: LUMO + 6	281: LUMO + 2
284: LUMO + 5	280: LUMO + 1
283: LUMO + 4	279: LUMO

278: HOMO	274: HOMO - 4
277: HOMO - 1	273: HOMO - 5
276: HOMO - 2	272: HOMO - 6
275: HOMO - 3	271: HOMO - 7

Excited State 1: Singlet-A 2.1997 eV 563.65 nm $f=0.0000$ $\langle S^{**2} \rangle=0.000$
 268 → 279 0.15064
 273 → 280 -0.12078
 276 → 280 -0.38944
 278 → 279 0.51709

Excited State 2: Singlet-A 2.2362 eV 554.44 nm $f=0.0878$ $\langle S^{**2} \rangle=0.000$
 268 → 280 0.15456
 273 → 279 -0.12315
 276 → 279 -0.39594
 278 → 280 0.50978

Excited State 3: Singlet-A 2.4841 eV 499.11 nm $f=0.6019$ $\langle S^{**2} \rangle=0.000$
 267 → 279 0.18411
 271 → 280 0.15414
 275 → 280 0.37053
277 → 279 0.50859
 278 → 281 0.10416

Excited State 4: Singlet-A 2.5194 eV 492.13 nm $f=0.0032$ $\langle S^{**2} \rangle=0.000$
 267 → 280 0.18342
 271 → 279 0.15357
 275 → 279 0.37564
 277 → 280 0.50077
 278 → 282 0.11763

Excited State 5: Singlet-A 2.8298 eV 438.13 nm $f=0.0167$ $\langle S^{**2} \rangle=0.000$
 272 → 280 0.46344
 273 → 280 0.10722

$274 \rightarrow 279$ 0.48517

Excited State 6: Singlet-A 2.8307 eV 438.00 nm $f=0.0000$ $\langle S^{**2} \rangle=0.000$
 $272 \rightarrow 279$ 0.46679
 $273 \rightarrow 279$ 0.10803
 $274 \rightarrow 280$ 0.48042

Excited State 7: Singlet-A 3.0120 eV 411.63 nm $f=0.0001$ $\langle S^{**2} \rangle=0.000$
 $265 \rightarrow 280$ 0.48777
 $266 \rightarrow 279$ 0.48917

Excited State 8: Singlet-A 3.0121 eV 411.62 nm $f=0.0032$ $\langle S^{**2} \rangle=0.000$
 $265 \rightarrow 279$ 0.48934
 $266 \rightarrow 280$ 0.48757

Excited State 9: Singlet-A 3.3329 eV 372.00 nm $f=0.3670$ $\langle S^{**2} \rangle=0.000$
 $268 \rightarrow 281$ 0.11900
 $275 \rightarrow 284$ -0.11071
 $276 \rightarrow 282$ -0.35666
 $277 \rightarrow 279$ -0.10923
 $277 \rightarrow 283$ -0.14334
 $278 \rightarrow 281$ 0.51153

Excited State 10: Singlet-A 3.3493 eV 370.18 nm $f=0.0020$ $\langle S^{**2} \rangle=0.000$
 $268 \rightarrow 282$ 0.11660
 $275 \rightarrow 283$ -0.12154
 $276 \rightarrow 281$ -0.35298
 $277 \rightarrow 280$ -0.11793
 $277 \rightarrow 284$ -0.15785
 $278 \rightarrow 282$ 0.50558

Excited State 11: Singlet-A 3.3972 eV 364.96 nm $f=0.0000$ $\langle S^{**2} \rangle=0.000$
 $267 \rightarrow 281$ 0.13985
 $271 \rightarrow 282$ 0.11924
 $275 \rightarrow 282$ 0.29330
 $276 \rightarrow 284$ 0.23196
 $277 \rightarrow 281$ 0.40854
 $278 \rightarrow 283$ -0.31076

Excited State 12: Singlet-A 3.3992 eV 364.74 nm $f=0.0480$ $\langle S^{**2} \rangle=0.000$
 $267 \rightarrow 282$ 0.13766
 $271 \rightarrow 281$ 0.11748
 $275 \rightarrow 281$ 0.28929
 $276 \rightarrow 283$ 0.23637
 $277 \rightarrow 282$ 0.40180
 $278 \rightarrow 284$ -0.31667

Excited State 13: Singlet-A 3.5445 eV 349.80 nm $f=0.0000$ $\langle S^{**2} \rangle = 0.000$

269 → 280 -0.35087
270 → 279 0.38225
272 → 282 0.13371
274 → 281 0.13899
276 → 280 -0.23875
278 → 279 -0.28913
278 → 283 -0.10241

Excited State 14: Singlet-A 3.5478 eV 349.47 nm $f=0.0003$ $\langle S^{**2} \rangle = 0.000$

269 → 279 -0.36282
270 → 280 0.37896
272 → 281 0.13862
274 → 282 0.14382
276 → 279 -0.21625
278 → 280 -0.27226
278 → 284 -0.14122

Excited State 15: Singlet-A 3.6108 eV 343.37 nm $f=0.0000$ $\langle S^{**2} \rangle = 0.000$

268 → 279 -0.19571
269 → 280 -0.20260
270 → 279 0.13356
275 → 282 -0.13628
276 → 280 0.34079
276 → 284 0.15993
277 → 281 -0.15335
278 → 279 0.33050
278 → 283 -0.21728

Excited State 16: Singlet-A 3.6199 eV 342.51 nm $f=0.0003$ $\langle S^{**2} \rangle = 0.000$

268 → 280 -0.23320
269 → 279 -0.24801
270 → 280 0.16062
272 → 281 0.11581
274 → 282 0.12126
276 → 279 0.39885
278 → 280 0.38127

Excited State 17: Singlet-A 3.6322 eV 341.35 nm $f=0.0000$ $\langle S^{**2} \rangle = 0.000$

268 → 279 -0.15382
269 → 280 -0.17357
270 → 279 0.12239
275 → 282 0.16666
276 → 280 0.17945
276 → 284 -0.25382
277 → 281 0.26673
278 → 279 0.14300

$278 \rightarrow 283$ 0.35857

Excited State 18: Singlet-A 3.6397 eV 340.65 nm $f=0.1397$ $\langle S^{**2} \rangle = 0.000$

$267 \rightarrow 282$ 0.11643
 $268 \rightarrow 284$ 0.10619
 $275 \rightarrow 281$ 0.22289
 $276 \rightarrow 283$ -0.28948
 $277 \rightarrow 282$ 0.31372
 $278 \rightarrow 284$ 0.40418

Excited State 19: Singlet-A 3.7035 eV 334.78 nm $f=0.1238$ $\langle S^{**2} \rangle = 0.000$

$267 \rightarrow 283$ 0.17844
 $271 \rightarrow 284$ 0.14715
 $275 \rightarrow 280$ 0.10411
 $275 \rightarrow 284$ 0.34065
 $277 \rightarrow 279$ -0.19132
 $277 \rightarrow 283$ 0.46033
 $278 \rightarrow 281$ 0.11975

Excited State 20: Singlet-A 3.7139 eV 333.84 nm $f=0.0006$ $\langle S^{**2} \rangle = 0.000$

$267 \rightarrow 284$ 0.17708
 $271 \rightarrow 283$ 0.14616
 $275 \rightarrow 283$ 0.33880
 $276 \rightarrow 281$ -0.10569
 $277 \rightarrow 280$ -0.20078
 $277 \rightarrow 284$ 0.45801
 $278 \rightarrow 282$ 0.13846

Excited State 21: Singlet-A 3.8032 eV 326.00 nm $f=0.0008$ $\langle S^{**2} \rangle = 0.000$

$267 \rightarrow 280$ 0.19502
 $275 \rightarrow 279$ 0.45438
 $275 \rightarrow 283$ -0.10817
 $277 \rightarrow 280$ -0.41880
 $277 \rightarrow 284$ -0.15788
 $278 \rightarrow 282$ -0.10349

Excited State 22: Singlet-A 3.8110 eV 325.33 nm $f=0.0763$ $\langle S^{**2} \rangle = 0.000$

$267 \rightarrow 279$ 0.20243
 $275 \rightarrow 280$ 0.45100
 $275 \rightarrow 284$ -0.11215
 $277 \rightarrow 279$ -0.41420
 $277 \rightarrow 283$ -0.16421
 $278 \rightarrow 281$ -0.10807

Excited State 23: Singlet-A 4.0483 eV 306.26 nm $f=0.0004$ $\langle S^{**2} \rangle = 0.000$

$269 \rightarrow 279$ 0.12842
 $270 \rightarrow 280$ -0.16548

272 → 281	0.35093
273 → 279	0.17956
274 → 282	0.36152
276 → 279	-0.16045
277 → 288	-0.13840
278 → 289	-0.15538

Excited State 24: Singlet-A 4.0502 eV 306.12 nm $f=0.0001$ $\langle S^{**2} \rangle = 0.000$

269 → 280	0.13860
270 → 279	-0.17996
272 → 282	0.37486
273 → 280	0.14600
274 → 281	0.38785
276 → 280	-0.17421

Excited State 25: Singlet-A 4.0883 eV 303.27 nm $f=0.0044$ $\langle S^{**2} \rangle = 0.000$

268 → 280	0.11871
269 → 279	0.11841
272 → 281	0.20855
273 → 279	-0.18100
274 → 282	0.21670
277 → 288	0.32601
278 → 289	0.36146

Excited State 26: Singlet-A 4.0990 eV 302.47 nm $f=0.0006$ $\langle S^{**2} \rangle = 0.000$

271 → 279	0.20136
271 → 287	-0.11342
273 → 291	0.11361
277 → 289	0.39442
278 → 288	0.43789

Excited State 27: Singlet-A 4.1212 eV 300.84 nm $f=0.0001$ $\langle S^{**2} \rangle = 0.000$

256 → 280	0.12524
260 → 279	-0.16056
262 → 279	-0.12784
263 → 280	-0.17687
264 → 280	-0.12542
268 → 279	-0.23535
269 → 280	-0.12221
272 → 282	-0.18064
273 → 280	0.26532
274 → 281	-0.19147
276 → 280	-0.26041
277 → 291	-0.10704
278 → 287	-0.17745

Excited State 28: Singlet-A 4.1759 eV 296.91 nm $f=0.1259$ $\langle S^{**2} \rangle = 0.000$

256 → 279	-0.13651
258 → 280	0.10441
260 → 280	0.15909
262 → 280	0.11986
263 → 279	0.18706
264 → 279	0.13177
268 → 280	0.22388
273 → 279	-0.23763
276 → 279	0.26755
277 → 288	-0.23070
278 → 289	-0.25928

Excited State 29: Singlet-A 4.2084 eV 294.61 nm $f=0.0001$ $\langle S^{**2} \rangle=0.000$

269 → 282	0.12141
270 → 281	-0.11113
272 → 284	0.44869
273 → 284	0.10391
274 → 283	0.46596

Excited State 30: Singlet-A 4.2087 eV 294.59 nm $f=0.0000$ $\langle S^{**2} \rangle=0.000$

269 → 281	0.12231
270 → 282	-0.11271
272 → 283	0.45090
273 → 283	0.10440
274 → 284	0.46798

Excited State 31: Singlet-A 4.2522 eV 291.57 nm $f=0.0737$ $\langle S^{**2} \rangle=0.000$

255 → 280	0.11899
257 → 279	0.15801
261 → 279	0.12692
263 → 280	-0.12061
264 → 280	0.17188
267 → 279	0.24589
271 → 280	0.43520
275 → 280	-0.31477

Excited State 32: Singlet-A 4.2612 eV 290.96 nm $f=0.0001$ $\langle S^{**2} \rangle=0.000$

265 → 282	0.47791
266 → 281	0.47786

Excited State 33: Singlet-A 4.2612 eV 290.96 nm $f=0.0004$ $\langle S^{**2} \rangle=0.000$

265 → 281	0.47767
266 → 282	0.47724

Excited State 34: Singlet-A 4.2728 eV 290.17 nm $f=0.0001$ $\langle S^{**2} \rangle=0.000$

255 → 279	0.11385
-----------	---------

257 → 280	0.15158
261 → 280	0.11591
263 → 279	-0.11902
264 → 279	0.16666
267 → 280	0.23230
271 → 279	0.40421
275 → 279	-0.30018
277 → 289	-0.15387
278 → 288	-0.17451

Excited State 35: Singlet-A 4.2941 eV 288.73 nm $f=0.0000$ $\langle S^{**2} \rangle=0.000$

273 → 280	0.17266
276 → 280	-0.11220
276 → 290	0.21735
277 → 291	0.26162
278 → 279	0.10794
278 → 287	0.47105

Excited State 36: Singlet-A 4.5003 eV 275.50 nm $f=0.0004$ $\langle S^{**2} \rangle=0.000$

268 → 282	-0.12004
270 → 282	-0.10882
276 → 281	0.49960
278 → 282	0.42714

Excited State 37: Singlet-A 4.5015 eV 275.43 nm $f=0.0515$ $\langle S^{**2} \rangle=0.000$

268 → 281	-0.11999
270 → 281	-0.10846
276 → 282	0.50209
278 → 281	0.42199

Excited State 38: Singlet-A 4.5232 eV 274.11 nm $f=0.0003$ $\langle S^{**2} \rangle=0.000$

265 → 284	0.48554
266 → 283	0.48546

Excited State 39: Singlet-A 4.5233 eV 274.10 nm $f=0.0004$ $\langle S^{**2} \rangle=0.000$

265 → 283	0.48757
266 → 284	0.48735

Excited State 40: Singlet-A 4.5362 eV 273.32 nm $f=0.2984$ $\langle S^{**2} \rangle=0.000$

256 → 279	0.12078
258 → 280	-0.32166
259 → 279	0.41485
260 → 280	0.28685
273 → 279	0.12375
277 → 282	0.10600
278 → 284	0.11216

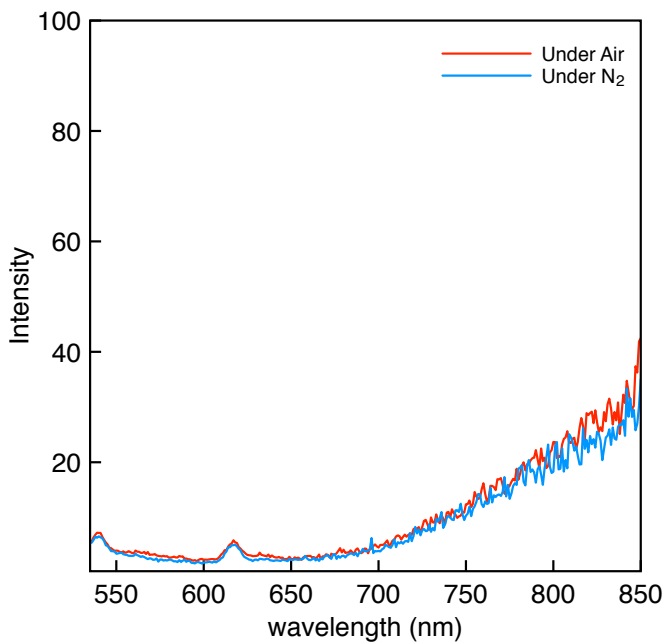


Fig. S15 Photoluminescence spectra of **1** measured in CH₂Cl₂ ($c = 0.020$ mM) excited at 520 nm under Air and N₂.

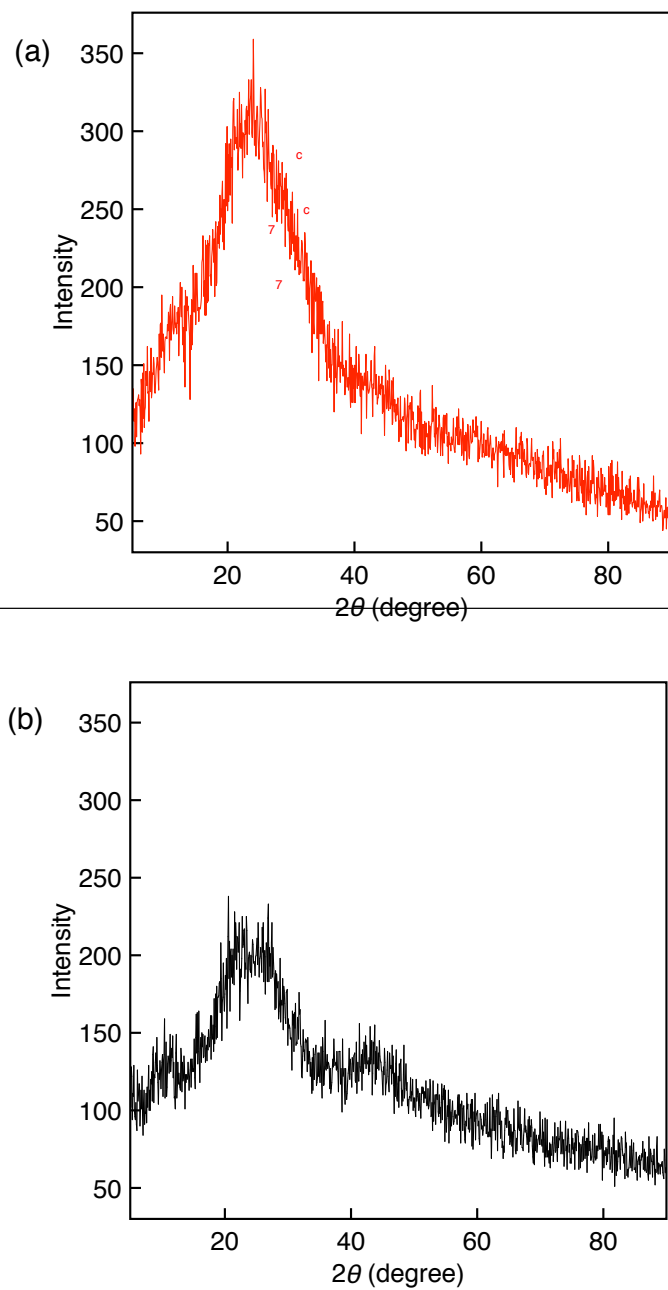


Fig. S16 XRD patterns of (a) **1** and (b) **1'** with Cu-K α radiation,

References

- S1) P. R. Florindo, D. M. Pereira, P. M. Borralho, P. J. Costa, M. F. M. Piedade, C. M. P. Rodrigues and A. C. Fernandes, *Dalton Trans.*, 2016, **45**, 11926–11930.
- S2) E. A. Glik, S. Kinayyigit, K. L. Ronayne, M. Towrie, I. V. Sazanovich, J. A. Weinstein and F. N. Castellano, *Inorg. Chem.*, 2008, **47**, 6974–6983.
- S3) T. Zhao, Z. Liu, Y. Song W. Xu, D. Zhang and D. Zhu, *J. Org. Chem.*, 2006, **71**, 7422–7432.
- S4) Z. He, G. Lai, Z. Li, X. Yuan, Y. Shen and C. Wang, *Chin. J. Chem.*, 2015, **33**, 550–558.
- S5) Y. Takihana, M. Shiotsuki, F. Sanda and T. Masuda, *Macromolecules*, 2004, **37**, 7578–7583.
- S6) M. Tabata, T. Fukushima, and Y. Sadahiro, *Macromolecules*, 2004, **37**, 4342–4350.
- S7) M. J. Frisch, G. W. Trucks, H. B. Schlegel, G. E. Scuseria, M. A. Robb, J. R. Cheeseman, G. Scalmani, V. Barone, G. A. Petersson, H. Nakatsuji, X. Li, M. Caricato, A. V. Marenich, J. Bloino, B. G. Janesko, R. Gomperts, B. Mennucci, H. P. Hratchian, J. V. Ortiz, A. F. Izmaylov, J. L. Sonnenberg, D. Williams-Young, F. Ding, F. Lipparini, F. Egidi, J. Goings, B. Peng, A. Petrone, T. Henderson, D. Ranasinghe, V. G. Zakrzewski, J. Gao, N. Rega, G. Zheng, W. Liang, M. Hada, M. Ehara, K. Toyota, R. Fukuda, J. Hasegawa, M. Ishida, T. Nakajima, Y. Honda, O. Kitao, H. Nakai, T. Vreven, K. Throssell, J. A. Montgomery, J. E. Jr., Peralta, F. Ogliaro, M. J. Bearpark, J. J. Heyd, E. N. Brothers, K. N. Kudin, V. N. Staroverov, T. A. Keith, R. Kobayashi, J. Normand, K. Raghavachari, A. P. Rendell, J. C. Burant, S. S. Iyengar, J. Tomasi, M. Cossi, J. M. Millam, M. Klene, C. Adamo, R. Cammi, J. W. Ochterski, R. L. Martin, K. Morokuma, O. Farkas, J. B. Foresman and D. J. Fox, Gaussian, Inc., Wallingford CT, 2019.
- S8) M. D. Hanwell, D. E. Curtis, D. C. Lonie, T. Vandermeersch, E. Zurek and G. R. Hutchison, *J. Cheminform.*, 2012, **4**, 17.